Int J Adv Manuf Technol (2018) 94:2125–2136
DOI 10.1007/s00170-017-1033-3

ORIGINAL ARTICLE

Probabilistic methodology for predicting the dispersion of residual stresses and Almen intensity considering shot peening process uncertainties

A. Atig[1,2] · R. Ben Sghaier[1,2] · R. Seddik[1] · R. Fathallah[1]

Received: 28 June 2017 / Accepted: 24 August 2017 / Published online: 5 September 2017

Abstract To ensure a high fatigue life and a reduced weight of automotive suspension system components, compressive residual stresses are commonly induced near the surface using many mechanical surface treatments. Among the most preferred techniques, shot peening process presents a high efficiency and a relative low cost. Nevertheless, the employment of such process is generally affected by many sources of variability. Indeed, the experimental residual stress measurements exhibit a significant variation from one component to another and even from different positions on the same component. Therefore, error bars are commonly used to quantify the variability of experimental residual stress measurements. Nevertheless, the majority of predictive approaches of residual stresses induced by shot peening do not consider the effect of the variability of shot peening process parameters. In this study, a probabilistic methodology is applied to evaluate the variability of the induced residual stress profile and the Almen intensity, regarding the scattering of the most significant shot peening process parameters. Furthermore, iso-probabilistic residual stress profile can be utilized to predict the shot peening residual stress profile with a specified probability of appearance.

Keywords Shot peening process · Probabilistic study · Monte Carlo simulation method · Iso-probabilistic residual stress profile

✉ A. Atig
akram.atig@gmail.com

[1] Ecole Nationale d'Ingénieurs de Sousse, BP 264 Sousse Erriadh, Université de Sousse, Sousse, Tunisia

[2] Institut Supérieur des Sciences Appliquées et de Technologie de Sousse, Rue Tahar Ben Achour Sousse, Université de Sousse, Sousse, Tunisia

1 Introduction

Shot peening process is a mechanical surface treatment extensively employed, in the spring manufacturing and the automotive industry, to enhance the fatigue behavior of metallic components subjected to cyclic loading [1, 2]. This cold surface treatment involves bombarding the surface of the metallic parts with small spherical shots, generally made of hard steel, at relatively high velocities (20–100 ms^{-1}) [3, 4]. The impact of a shot particle generates a compressive residual stress field and a plastic deformation in the near surface region [5]. Furthermore, this process may increase the near surface hardness due to the surface work hardening effect [6]. Nevertheless, shot peening may induce unfavorable effects on the component surface such as the intensification of the surface roughness and the creation of a local surface damage (micro-cracks, scaling and overlaps) [6, 7]. In order to enhance the magnitude of the favorable effects and to restrict the unfavorable effects, it is necessary to control the effectiveness and repeatability of shot peening process. Among the most important control factors, we found the peening coverage and the Almen intensity. The first parameter describes the proportion of the surface covered, at least once, with indents, to the total treated area. The second parameter is essentially linked to the stream energy transmitted upon impingement [8]. This energy is mainly related to the velocity, the size, the shape and the density of the projectile [9]. To measure the Almen intensity, Almen standard size strips (A, N and C), made of SAE1070 spring steel, are used in the shot peening process. The Almen strip test, which involves measuring the arc height of the deflected strip, was suggested by Almen and Black [10]. Detailed procedures and specifications can be found in SAE-J442, SAE-J443 [11, 12].

It has been well recognized that the total production cost of leaf springs presents an important factor during the design

stage. Nevertheless, the acquisition of the raw spring material with a reduced price generates a considerable variability of their mechanical and metallurgical characteristics [13, 14]. Furthermore, the shot quality and size may not be guaranteed for suitable acquisition costs. Thus, the scattering of many design parameters, related to mechanical raw material properties and the shot peening process conditions, may take the experimental shot peening investigations away from the predicted results [15]. Therefore, leaf spring designers seek to incorporate the effects of uncertainties into the applied design approach [13].

Among the main sources of uncertainty are the variability in size of the projectile. This parameter requires a high quality of control and inspection [15, 16]. The SAE J444 specification recommends cast steel shot size specifications in terms of sieving results [17]. The nominal size of the shot media, proposed by specification SAE J444, is a fixed value while the real samples enclose a range of shot sizes. This variability is related to both the production stage and the sieve analysis procedure [16]. Indeed, a practical production method consists on pouring a stream of liquid steel into high-pressure water jets in order to obtain round particles after solidification stage. Then, the poorly formed particles are removed. Later, the remaining particles are adjusted by sieving and classified by size.

Besides, the media velocity has a high variability during the shot peening process. The effective velocity distribution of shots impacting the treated surface cannot be accurately inspected. The shot peening devices present the main cause of shot speed variability. This primordial shot peening parameter is generally correlated to the Almen intensity and the shot size [8, 18]. Therefore, the variability of the shot size and speed affects the measured Almen intensity values.

It is well established that the shot peening process shows a high dispersion of the residual stress experimental results. This scattering is generally related to an inherent variability of many significant parameters. These significant parameters can be classified into three groups: (i) variables related to the shot stream such as the size, the shape, the hardness, the density velocity, the impact angle, and the peening time; (ii) variables related to the treated part such as the mechanical properties, the elastic-plastic behavior, and the geometric details; and (iii) parameters describing the contact conditions such as the restitution and the of friction coefficients [19]. The probabilistic distributions shot peening results can be evaluated by using diverse approximation and numerical probabilistic approaches such as the Monte Carlo simulation technique. Besides the straightforward implementation, the classical Monte Carlo simulation technique is considered as an efficient and robust tool when dealing with an analytical model that describes the relation between the input parameters and the outcomes [20, 21]. This powerful technique is used to perform a large number of simulation samples and provides a numerical approximation of the model outcome distributions. Then, it is easy to characterize the distribution of each probabilistic output parameter.

In addition to the analytical and the numerical models, mathematical modeling using response surface techniques have been widely used to construct efficient shot peening models [22, 23]. Moreover, artificial intelligence, based on artificial neural network method, has been utilized to develop a mathematical model of shot peening process [24–26]. The obtained model is useful to predict and optimize a high number of the shot peening process outputs.

Numerical simulations using FE software are extensively used to predict the shot peening modifications [3, 4]. Seddik et al. [27, 28] proposed a multi-shot dynamic finite element model, based on Frija et al. [29] and Taehyung et al. [30] models, to simulate the shot-peening process. Hassani-Gangaraj et al. [31, 32] suggested a hybrid approach, based on Bagherifard et al.'s [33] work, which combines finite element simulation of peening process with the dislocation density model. The proposed approach simulated severe shot peening process to induce a surface nano-crystallization. Recently, alternative approaches using the discrete element method (DEM) coupled with the finite element method (FEM) have been carried out to simulate the real shot peening process with a reduced computational effort [4, 34].

It should be noted that numerical models based on the finite element methodology present a powerful tool to simulate a real shot peening process. However, for probabilistic studies which require a high number of mechanical model calls (10^4–10^5), time-consuming models are not preferred. Therefore, analytical models present an interesting solution for studying the effect of uncertainties on shot peening process. Many analytical models of shot peening process have been presented in the literature. First of all, Al-Hassani [5] proposed a predictive model based on empirical formulations related to experimental measurements. Next, Fathallah et al. [19] proposed an extension of the model developed by Guechichi et al. [35] and improved by Khabou et al. [36], by the integration of the effects of the tangential friction and the hardness ratio between the shot and the treated material. In the same context, Shen and Alturi [37] proposed a simplified model based on the Al-Hassani [5] and Li et al. [38] models to estimate the residual stresses. Then, the latter model has been completed by Miao et al. [39] to predict the Almen intensity and the residual stress distribution for Almen strip. Recently, many studies have been developed to improve Li's model by considering different stress-strain constitutive laws for the treated material [40–43].

In this paper, the theoretical model proposed by Li et al., enhanced by Shen and Alturi and completed by Miao et al., has been adopted to study the effect of the variability of the shot peening conditions and the treated material parameters on the Almen intensity and the compressive residual stress profile. The evaluation of shot peening process outcomes has

been performed using the Monte Carlo simulation technique. This inherent variability may affect the experimental results. Therefore, it is very interesting to associate to the predicted residual stress profile, a theoretical error bar. The proposed probabilistic study allows the estimation of the variability of the shot peening outcomes based on the variability of the process factors.

2 Analytical modeling of compressive residual stress after shot peening

2.1 Single shot impact analysis based on hertz contact theory

In this study, the simplified mechanical shot peening model developed by Li et al. and enhanced by Shen et al. and Miao et al. has been adopted. This model adopts the Hertzian elastic theory of contact for the elastic stress computation. The contact is considered between an elastic sphere and an elastic semi-infinite space. The elastic stress tensor during the contact reach their maximum along the z-axis passing through the center O of the contact area in the target body, where the stresses can be expressed according to the Hertzian contact theory as follows:

$$\sigma_x^e(z) = \sigma_y^e(z) = -{p_0}^*\left[-\frac{1}{2}A(z) + (1+\nu)B(z)\right] \tag{1}$$

$$\sigma_z^e(z) = -{p_0}^* A(z) \tag{2}$$

with

$$A(z) = \left[1 + \left(\frac{z}{a_e}\right)^2\right]^{-1} \tag{3}$$

and

$$B(z) = 1 - \frac{z}{a_e}\tan^{-1}\left(\frac{a_e}{z}\right) \tag{4}$$

${p_0}^*$ and ${a_e}^*$ are, respectively, the maximal elastic pressure at the center of the contact area and the maximal radius of the elastic contact circle. They can be obtained using the following equations:

$${p_0}^* = \frac{1}{\pi}\left(40\pi k\rho E_H^4 (V\sin\theta)^2\right)^{\frac{1}{5}} \tag{5}$$

$${a_e}^* = \frac{D}{2}\left[\frac{5}{4}\pi k\rho\frac{(V\cdot\sin\theta)^2}{E_H}\right]^{\frac{2}{5}} \tag{6}$$

where D, ρ, and V correspond, respectively, to the diameter, the density, and the velocity of the shot. θ presents the angle of impingement. k is an efficiency coefficient linked to the elastic and the thermal dissipation and is fixed at 0.8 according to Johnson [44].

E_H is the equivalent Young's modulus; it is given by:

$$\frac{1}{E_H} = \frac{1-\nu_s^2}{E_s} + \frac{1-\nu_T^2}{E_T} \tag{7}$$

where E_s and ν_s are the Young's modulus and the Poisson's ratio of the shot material and E_t and $\nu_t$are the Young's modulus and the Poisson's ratio of the target material.

2.2 Stress-stain study of the elastic contact

Once the principal elastic stresses are computed, the Von Mises equivalent stress σ_i^e can be obtained, as follows:

$$\sigma_i^e = \frac{1}{\sqrt{2}}\left[\left(\sigma_x^e - \sigma_y^e\right)^2 + \left(\sigma_y^e - \sigma_z^e\right)^2 + \left(\sigma_z^e - \sigma_x^e\right)^2\right] \tag{8}$$

According to Hooke's law, the Von Mises equivalent strain ε_i^e and the principal strains ε_x^e,ε_y^e, and ε_z^e in the target material are expressed as follows:

$$\varepsilon_i^e = \frac{\sigma_i^e}{E_T} \tag{9}$$

$$\varepsilon_x^e = \varepsilon_y^e = \frac{1}{E_T}\left[\sigma_x^e - \nu_T\left(\sigma_y^e + \sigma_z^e\right)\right] \tag{10}$$

$$\varepsilon_z^e = \frac{1}{E_T}\left[\sigma_z^e - 2\nu_T\sigma_x^e\right] \tag{11}$$

2.3 Elastic-plastic analysis of the loading process

To calculate the elastic-plastic strain from the elastic strain obtained from the contact theory of Hertz, Li et al. [38] introduced a straightforward method. First of all, the strain field is computed as if the material was purely elastic. Then, the plastic strain in the elastic-plastic deformation stage is obtained from the strain field produced by the purely elastic impact and from the characteristics of a perfectly plastic impact using an empirical formulation introducing an efficiency factor α as:

$$\varepsilon_i^p = \begin{cases} \varepsilon_i^e & for\ \ \varepsilon_i^e \le \varepsilon_s \\ \varepsilon_s + \alpha\left(\varepsilon_i^e + \varepsilon_s\right) & for\ \varepsilon_i^e > \varepsilon_s \end{cases} \tag{12}$$

The coefficient α is the ratio of the maximum plastic indentation ${a_p}^*$ to the maximum elastic contact radius ${a_e}^*$. The maximum plastic indentation can be written as

$$a_p = \frac{D}{2}\left[8\rho\frac{(V\cdot\sin\theta)^2}{9\sigma_s}\right]^{\frac{1}{4}} \tag{13}$$

After the computation of the elastic-plastic strains, the elastic-plastic stresses are carried out in accordance with the elastic-plastic stress-strain curve:

$$\sigma_i^p = \begin{cases} \sigma_i^e & for \quad \varepsilon_i^p \le \varepsilon_s \\ \sigma_s + H^1(\varepsilon_i^p + \varepsilon_s) & for \ \varepsilon_s \le \varepsilon_i^p < \varepsilon_b \\ \sigma_b & for \quad \varepsilon_i^p \ge \varepsilon_b \end{cases} \tag{14}$$

2.4 Trans-residual and residual stress calculation after unloading

The trans-residual stress is defined as the residual stress obtained on the treated target after the unloading of one single shot, and the calculation of the trans-residual is essential to obtain the induced residual stress which presents the residual stress of 100% shot peening coverage (full average).

Based on the following assumptions: (i) the material of the treated target has an isotropic hardening behavior, (ii) the amount of deformation induced by a shot is small, and (iii) unloading is an elastic process until the reversed yielding starts and that hydrostatic stresses do not induce a plastic deformation.

The trans-residual stresses are calculated from this equation:

$$\sigma_{ij}^t = \begin{cases} 0 & for \quad \sigma_i^e < \sigma_s \\ s_{ij}^p + s_{ij}^e & for \ \sigma_s \le \sigma_i^e \le 2\sigma_b \end{cases} \tag{15}$$

with s_{ij}^p the elastic-plastic stress deviators which can be obtained, according to the Ilyushin's [45] elastic-plastic theory, from the following relation:

$$S_{ij}^p = \frac{1}{1+\nu_T} \cdot \frac{\sigma_i^p}{\varepsilon_i^p} \cdot e_{ij}^p \tag{16}$$

The principal components of the deviatoric strain in elastic plastic domain are

$$e_x^p = e_y^p = \frac{1}{3}(1-\nu_T) \cdot \varepsilon_i^p \tag{17}$$

$$e_z^p = e_y^p = -\frac{2}{3}(1-\nu_T) \cdot \varepsilon_i^p = -2e_x^p \tag{18}$$

Thus, the elastic-plastic principal components of the deviatoric stress tensor are given by

$$S_x^p = S_y^p = \frac{1}{1+\nu_T} \cdot \frac{\sigma_i^p}{\varepsilon_i^p} \cdot e_x^p = \frac{1}{3}\sigma_i^p \tag{19}$$

$$S_z^p = -\frac{2}{3}\sigma_i^p = -2S_y^p \tag{20}$$

For the case of $\sigma_s \le \sigma_i^e \le 2 \cdot \sigma_i^p$, the elastic-plastic principal components are achieved from the following relations:

$$\sigma_x^t = \sigma_y^t = \frac{1}{3}\left(\sigma_i^p - \sigma_i^e\right) \tag{21}$$

$$\sigma_z^t = -2 \cdot \sigma_x^t \tag{22}$$

For the case of $\sigma_i^e \ge 2 \cdot \sigma_i^p$, the treated material will undergo a reversed yielding and hardening. Initially, a stress amount of $2 \cdot \sigma_i^p$ is elastically unloaded before a reversed yielding occurs. Nevertheless, a part of stresses could be confined. An increment of these unreleased stresses is expressed as

$$\Delta\sigma_i^e = \sigma_i^e - 2 \cdot \sigma_i^p \tag{23}$$

The increments of elastic and elastic-plastic strains can be calculated by the following relations:

$$\Delta\varepsilon_i^e = \frac{\Delta\sigma_i^e}{E} \tag{24}$$

$$\Delta\varepsilon_i^p = \alpha \cdot \Delta\varepsilon_i^e \tag{25}$$

The elastic-plastic stress increment is obtained based on multilinear stress-strain curve as follows:

$$\Delta\sigma_i^p = H^1 \cdot \Delta\varepsilon_i^p \tag{26}$$

when $\sigma_i^e \ge 2 \cdot \sigma_i^p$, the trans-residual stresses can be re-written as

$$\sigma_x^t = \sigma_y^t = \frac{1}{3}(\sigma_i^p - 2\sigma_i^p - \Delta\sigma_i^p) \tag{27}$$

$$\sigma_z^t = -2 \cdot \sigma_x^t \tag{28}$$

When the shot-peened surface is 100% covered by plastic indentation (full coverage), the deformation field is assumed to be steady and continuous and the target surface is assumed to hold back the plane state. Therefore, both $\varepsilon_x$and $\varepsilon_y$are considered as null and all tensors depend only on the depth z. Consequently, at full coverage, the following equilibrium conditions must be satisfied:

$$\sigma_x = \sigma_x = f(z) \tag{29}$$

$$\sigma_z = 0 \tag{30}$$

$$\varepsilon_x = \varepsilon_y = 0 \tag{31}$$

$$\varepsilon_z = f(z) \tag{32}$$

The trans-residual stresses do not satisfy the above-mentioned equilibrium conditions and must be partially relaxed. Regarding Hooke's law, the stresses associated to this relaxation process can be calculated as follows:

$$\sigma_x^{rel} = \sigma_y^{rel} = \frac{\nu}{1-\nu} \cdot \sigma_z^t \tag{33}$$

Finally, the induced stresses related to full coverage are depicted as

$$\sigma_x^{ind} = \sigma_y^{ind} = \sigma_x^t - \sigma_x^{rel} = \frac{1+\nu}{1-\nu}\sigma_x^t \tag{34}$$

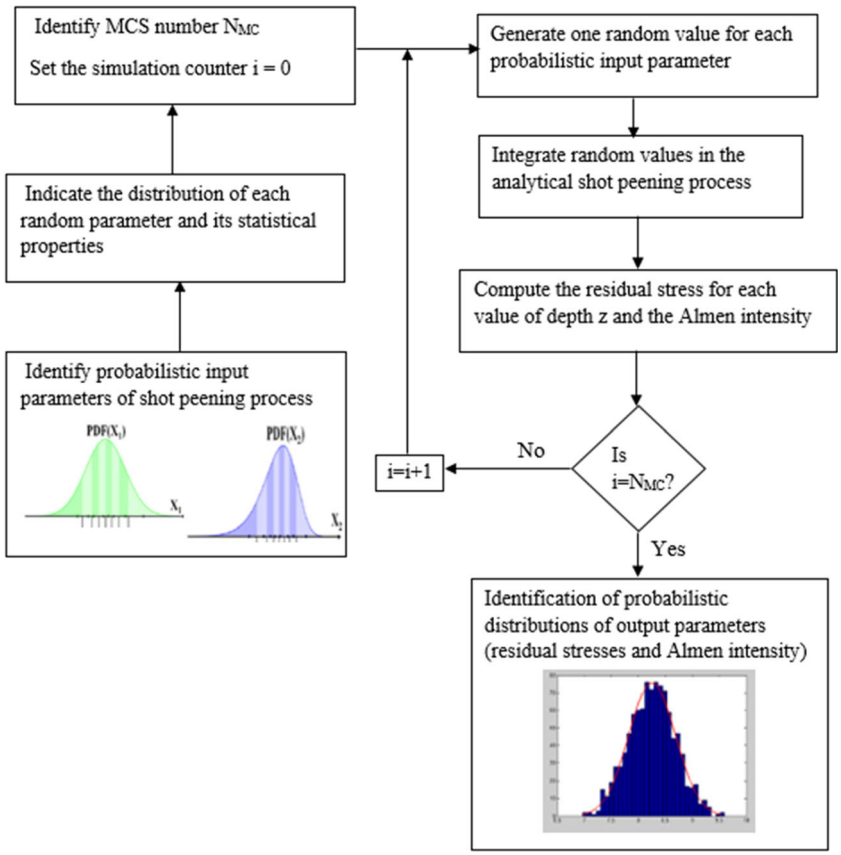

Fig. 1 Flowchart of Monte Carlo simulation of shot peening process outcomes

2.5 Calculation of residual stress for thin target component

The shot peened of thin component generate a redistribution and self-equilibrium of the compressive induced stress. A stretching force F_x and a bending moment M_x are created after shot peening. For that reason, the release of the Almen strip from the support and bolts after shot peening will cause the stretching and the bending of the initially flat strip. Hence, the equilibrium conditions are expressed as

$$\int_0^h \sigma_x^{ind} b{\cdot}dz + F_x = 0 \tag{35}$$

$$\int_0^h \sigma_x^{ind} \left(\frac{h}{2} - z\right) b{\cdot}dz + M_x = 0 \tag{36}$$

The residual stress distribution σ_x^{res}, for a thin target component (i.e., Almen strip), can be calculated by the following relation:

$$\sigma_x^{res} = \sigma_x^{ind} + \sigma_x^b + \sigma_x^s = \sigma_x^{ind} + \frac{F_x}{A} + \frac{M_x\left(\frac{h}{2} - z\right)}{I} \tag{37}$$

The stretching force effect is usually neglected and only the bending moment has a significant effect. To predict the arc height, a simplified relation is expressed as follows:

$$Archeight = \frac{3{\cdot}M_x{\cdot}{I_m}^2}{2{\cdot}E_T{\cdot}b{\cdot}h^3} \tag{38}$$

where I_m presents the reference distance for measuring Almen intensity.

Table 1 Mechanical properties of SAE 1070 spring steel [46]

SAE 1070 steel	Value
Young's modulus (GPa)	200
Yield strength (MPa)	1120
Ultimate tensile stress (MPa)	1270
Poisson's ratio	0.31
Elongation at UTS (%)	8.2

Table 2 Material properties and size of different shot media

Shot and material properties	Value		
Young's modulus (GPa)	210		
Density (kg/m3)	7800		
Poisson's ratio	0.31		
Type of shot particles	S110	S170	S280
Diameter average (mm)	0.356	0.504	0.84

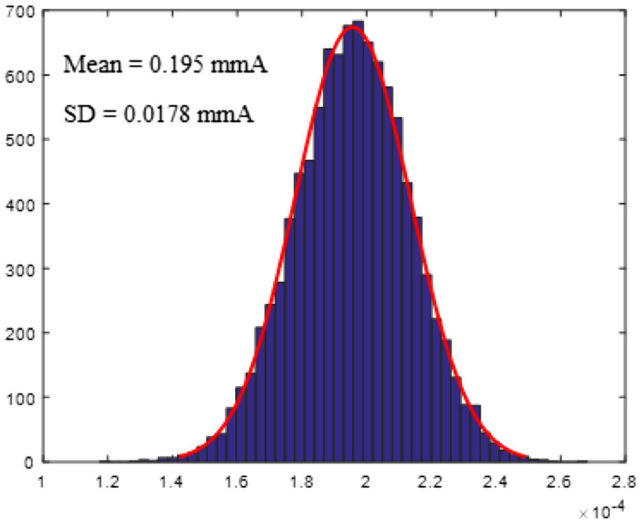

Fig. 2 Histogram and fitted probability density function of Almen intensity

3 Probabilistic modeling approach procedures

In this paper, we propose to study the effect of different sources of uncertainty (i.e., dispersion of shot peening conditions and material parameters) on the shot peening process results such as the compressive residual stresses and the Almen intensity. Therefore, a probabilistic shot peening model, used to assess the variability of the shot peening results, has been established. It should be noticed that the Monte Carlo simulation method is adopted to perform the statistical analysis. This technique is commonly used in probabilistic studies to assess the distribution of mechanical model outcomes based on a sampling of each random input parameter. Indeed, this method is employed to generate a high-dimension representative sample for each probabilistic input parameter according to its distribution law. Next, the sample values are incorporated to the mechanical model to obtain a probabilistic distribution of each model result. In this study, all random variables are assumed to follow a normal distribution characterized by mean and coefficient of variation (CoV) values. The flowchart describing the proposed approach is illustrated in Fig. 1. It presents the different suggested steps for computing the probabilistic distributions of Almen intensity and residual stress profile. To insure the convergence and the stability of the probabilistic results, a Monte Carlo number of 10^5 has been selected. In fact, it is found that 10^5 simulations satisfy a high level of accuracy with reasonable computational time.

4 Applications

4.1 Effect of shot size dispersion on the Almen intensity

The analytical shot peening model developed by Li et al. [38] and enhanced by Shen et al. [37] and Miao et al. [39] presents a simplified and efficient procedure to calculate the induced stresses. Based on the obtained induced stress profile, the Almen intensity may be performed using Eq. (38) introduced by Guagliano [46] and the bending equilibrium condition depicted by Eq. (36) which is introduced by Al-Hassani [5]. An Almen Strip A is a plate made of SAE 1070 spring steel with dimensions of 76 mm × 19 mm × 1.29 mm. It is frequently used to implement the Almen intensity. The Almen strip material behavior is assumed to have a bilinear elastic-plastic with isotropic hardening. Table 1 illustrates the mechanical properties of SAE 1070 spring steel.

The shot material behavior is considered as elastic. In this study, the effect of cast steel shot size dispersion on the Almen intensity has been investigated. It should be emphasized that the particles shape is assumed to be spherical and

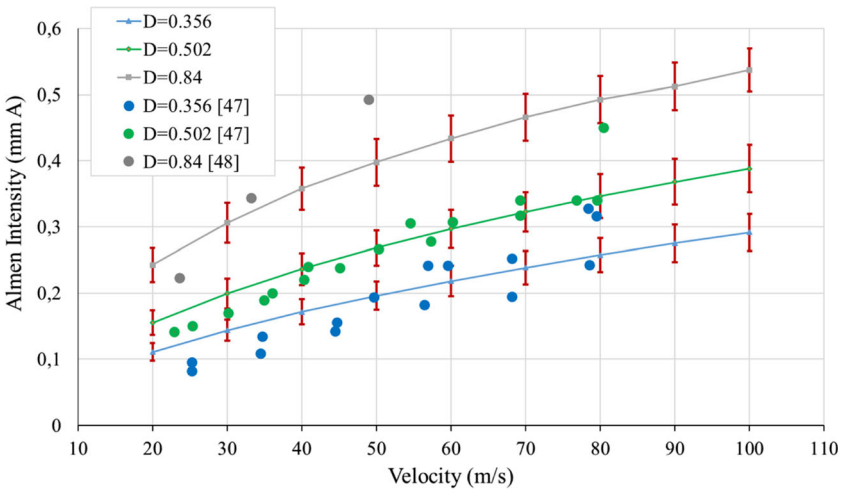

Fig. 3 Effect of 10% of shot size and velocity dispersions on the ALMEN intensity

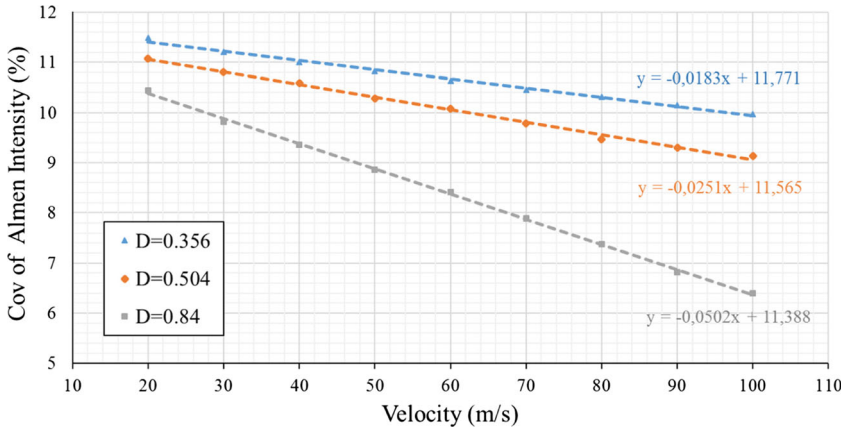

Fig. 4 Variation of ALMEN intensity dispersion regarding the velocity

characterized by its diameter. Table 2 depicts the material properties, types, and sizes of different shot media.

The shot particle size shows a potential scattering which is generally related to the production technique and the screening method. Since it is very difficult to quantify the size dispersion for a given particle batch, let us suppose that it follows a normal distribution characterized by diameter average and a CoV of 10%. In the same context, the impingement velocity is assumed to be normally distributed with a 10% of randomness. To compute the variability of the Almen intensity resulting from the above-mentioned dispersions, a large number of diameter and velocity samples have been carried out according to their probabilistic distributions. Next, the analytical model is simulated for each couple of shot size and velocity random values. Consequently, a sample of Almen intensity values is obtained. In this step, the corresponding distribution type should be determined according to the obtained values of the Almen intensity sample.

Figure 2 shows the distribution of the Almen intensity data sample for the case of a shot diameter average of $D_{moy} = 0.356$ and a velocity of 50 m/s. It is found that the obtained empirical data distribution is well adapted to a normal distribution.

The normality of the Almen intensity distribution is verified by using Henry's line method, and a good coefficient of determination of 0.999 is obtained. The obtained Almen intensity values follow a normal distribution of a mean value of 0.195 mm A and a standard deviation of 0.0178 mm A, which presents a CoV of 9.12%.

Figure 3 shows the dispersion of the Almen intensity curve, for three different types of steel shots, regarding the shot velocity mean values, with a consideration of 10% of both the shot size and velocity dispersions. Actually, the randomness of Almen intensity is related essentially to the size, the velocity, and the density of shots [8]. It is observed that the proposed analytical results of Almen intensity are in good agreement with experimental investigations available in the literature[47–48]. Therefore, the experimental measurement variability may be explained by the randomness of shot peening conditions such as the shot size and velocity.

Figure 4 shows the variation of the Almen intensity CoV regarding the shot velocity for the three different cases of shot diameter average: $D_{moy} = 0.356$, $D_{moy} = 0.504$, and $D_{moy} = 0.84$. It is observed that the dispersion of the Almen intensity decreases linearly with high velocity. This diminishing becomes faster for high shot size. In fact, the CoV of Almen intensity decreases for the case of $D_{moy} = 0.84$, from 10.49% for a shot velocity of 20 m/s to 6.38% for a shot velocity of 100 m/s.

4.2 Effect of the dispersion of shot peening conditions and target material parameters on the residual stress profiles for 65Si7 spring steel

In this section, a comparison between the theoretical residual stresses and experimental residual stresses measured by Aggarwal and co-workers for the case of 65Si7 [49] has been performed. The treated material parameters are depicted in Table 3.

For the experimental shot peening conditions, a shot was made by cast steel with a diameter of 1 mm and an Almen intensity of 0.3 mm A. to implement the analytical residual stresses, an approximation of the shot velocity mean value is deducted from Fig. 4 with a previous knowledge of the media type and the Almen intensity. All input parameters of the

Table 3 Mechanical properties of SAE 60Si7 spring steel [49]

60Si7 spring steel	Value
Young's modulus (GPa)	210
Yield strength (MPa)	1147
Ultimate tensile stress (MPa)	1256
Poisson's ratio	0.29
Elongation at UTS (%)	10%

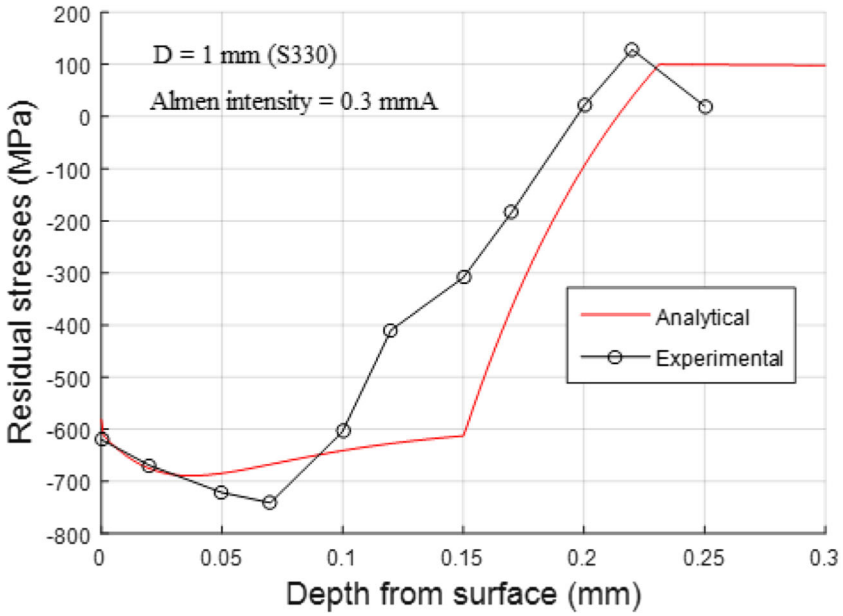

Fig. 5 Comparison of theoretical residual stress and experimental residual stress of 65Si7 spring [49]

analytical model are represented below: the shot-peened specimen has a rectangular section with 5 mm of depth and 13 mm of width [49] and the cast shot properties are the shot diameter $D_s = 1$ mm, the shot mass density $\rho_s = 7800 kg/m^3$, and the shot Poisson's ratio $\nu_s = 0.31$. For the shot conditions, the angle of impact $\theta = 75^{\circ}$ and the velocity $\theta = 25m \cdot s^{-1}$. Figure 5 includes both the experimental results developed by Aggarwal et al. and the adopted analytical model results. The adopted theoretical approach exhibits a good coherence with experimental measurements of residual stresses.

For the superficial layers, the analytical model predicts well the experimental results. However, for the deep layers, a slight shift has been observed. This alteration in high depth is primarily explained by the fact that the adopted model assumes that the residual stresses and plastic strains are uniformly distributed along the target specimen. However, the experimental procedure, which supplies a large number of passes, may provoke a high variability and a non-uniformity of the measured stresses and strains. This variability is often increased in deep layers.

The experimental residual stress profiles are commonly accompanied by error bars which may gather the measurement errors and the randomness of shot peening process. Nevertheless, the current analytical and numerical predictive models do not take into account such important information. Therefore, it is interesting to include, to the predictive models, a probabilistic approach that controls the unavoidable shot peening process uncertainties. Figure 6 presents the dispersion of the residual stress profile generated by a CoV of 2 and 5% of the target material parameters: the Young's modulus, the yield strength, ultimate tensile stress, Poisson's ratio, and elongation at UTS. This randomness of shot-peened material parameters generates a dispersion zone of the residual stress

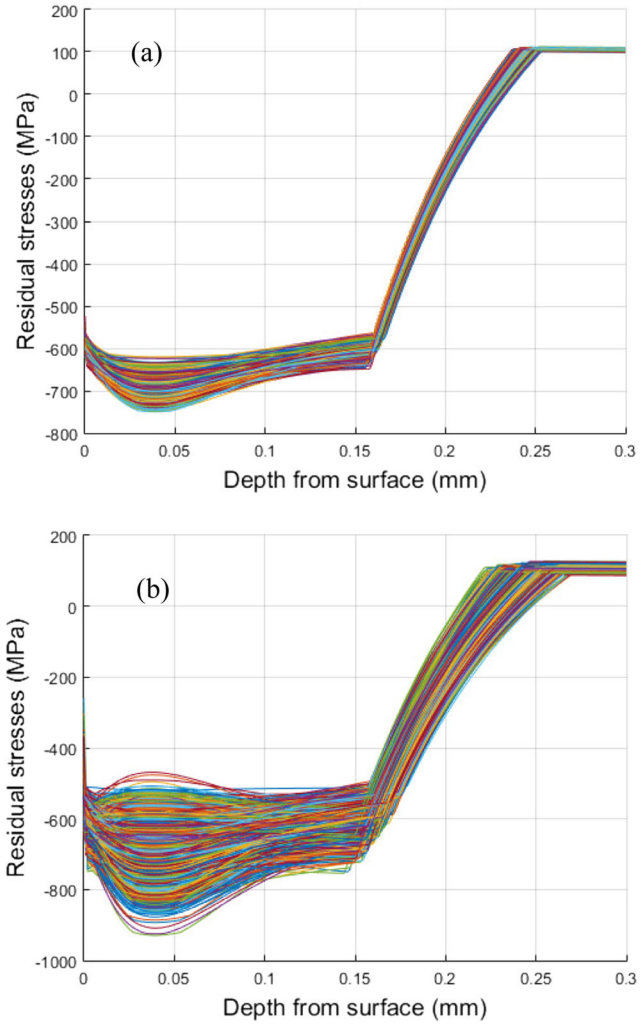

Fig. 6 The dispersion of analytical residual stress profile for a coefficient of variation of **a** 2 and **b** 5% of target material parameters

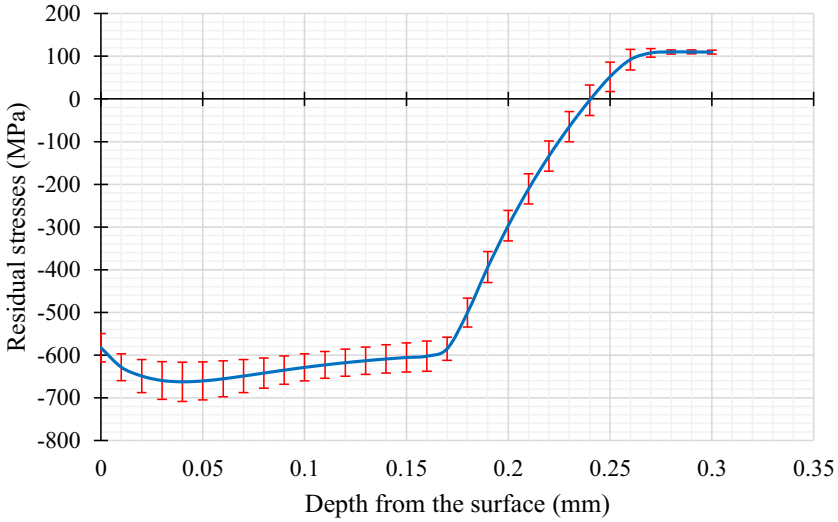

Fig. 7 Effect of 5% of leaf spring material dispersion on the residual stresses

profile which presents all the possible residual stress profiles. Next to a normality verification of obtained residual stresses, this scattering may be presented by the standard deviation of residual stresses for a given depth. Therefore, the description of the residual stress profile can be performed using the error bars of more or less a standard deviation value. Figures 7 and 8 present, respectively, the effect of 5% of spring steel materiel dispersions: the Young's modulus, the yield strength, ultimate tensile stress, Poisson's ratio, and elongation at UTS dispersions, and the effect of 5% of shot peening conditions' dispersions: the shot size, the velocity, and the impact angle dispersions on the residual stress profile. It is observed that the dispersion of the target material parameters affects all the residual stress profile. However, the scattering of shot peening conditions (the shot velocity, the shot size, and the angle of impact) has a significant effect only for deep layers. A maximal standard deviation of 46 MPa is obtained in a depth of 0.05 mm for the first case (5% of Leaf spring materiel dispersion). For the second studied case, the maximal standard deviation which reaches 106 MPa is obtained in a depth of 0.19 mm. Figures 9 and 10 show the 50, 90, and 99% iso-probabilistic residual stress profile for the cases of 2 and 5% of dispersion of, respectively, the target material parameters and the shot peening conditions. The 50% iso-probabilistic profile presents the deterministic profile. Ninety-nine percent iso-probabilistic profile provides the poorest possible case of compressive residual stress profiles when the effect of uncertainties is taken into account. For example, it is possible to have a surface residual stress of − 437 MPa for the case of a dispersion of 5% of material parameters while the deterministic predicted results propose a value of − 580 MPa. Therefore, when the sources of significant uncertainties on the shot peening process are quantified, 99% iso-probabilistic profile presents the efficient curve that should be taken into account for the fatigue design of shot-peened components. It is also remarkable in Fig. 9 that, for the cases of 2 and 5% of materiel

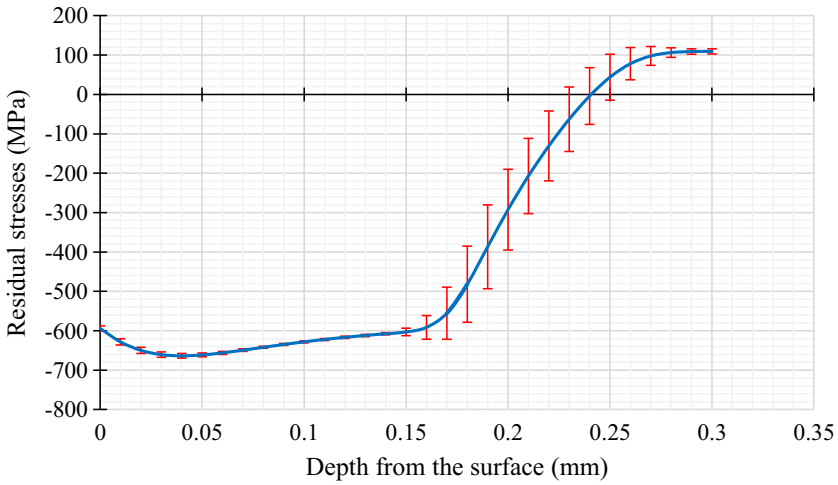

Fig. 8 Effect of 5% of shot peening conditions on the residual stresses

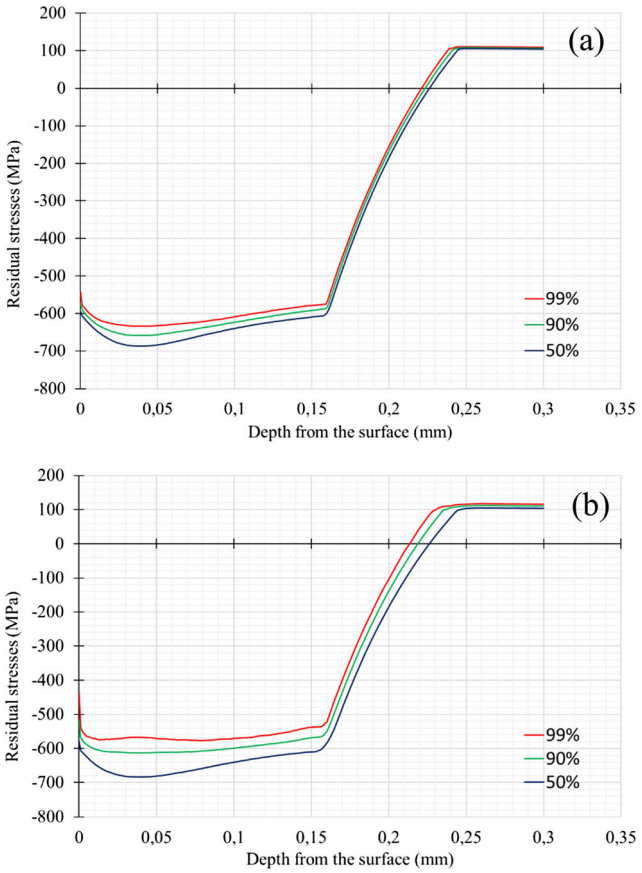

Fig. 9 Iso-probabilistic residual stress curves for **a** 2 and **b** 5% of dispersion of treated material parameters

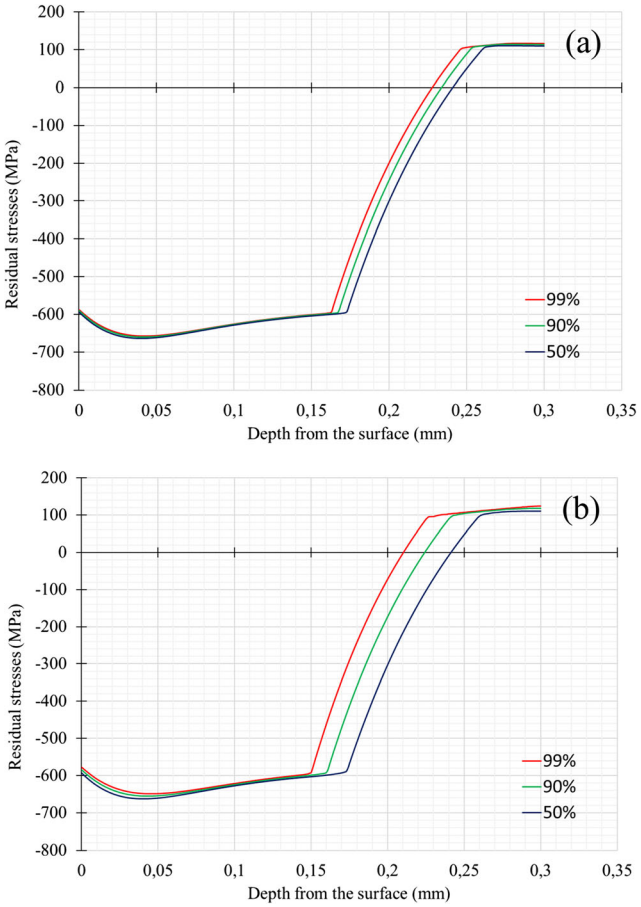

Fig. 10 Iso-probabilistic residual stress curves for **a** 2 and **b** 5% of shot peening process condition variability

input parameters' dispersions, the 99% surface residual stress increase respectively from − 542 to − 437 MPa. As shown in Fig. 10, the dispersions of 2% of the shot size, the shot velocity, and the impact angle have no significant effect on the surface residual stress and a slight effect for the case of 5% of dispersions of the aforementioned parameters. However, the shot peening conditions' dispersion has a significant effect on the depth of affected layers. In fact, for the case of 5% of variability, the depth at zero stress vary from 0.24 mm for a probability of 50% to 0.21 mm for a probability of 99%.

5 Conclusion

In this study, a predictive model of compressive residual stress proposed by Li et al. [38] and enhanced by Shen et al. [37] and Miao et al. [39] has been reviewed. Next, a probabilistic methodology has been developed, based on the above-mentioned model, to incorporate the effects of shot peening process parameters' dispersions on both Almen intensity and compressive residual stress profile. The proposed approach has been applied to assess randomness of Almen intensity for 10% of shot size and velocity randomness. A comparison of calculated Almen intensity values with available investigations shows a good coherence. It is noticed that the proposed approach is able to give reasonable probabilistic results compared to experimental Almen intensity dispersion.

Moreover, the suggested probabilistic approach has been applied for the case of 65Si7 to quantify the scattering of the predicted compressive residual stress profile with consideration of the randomness of both the mechanical properties of the treated material and the shot peening conditions. The predicted residual stress profile displays a considerable accuracy by assessing its variability due to many inherent sources of randomness. In addition, the iso-probabilistic residual stress profiles of 50, 90, and 99% have been implemented. The latter profile guarantees that all random residual stress results are better than those predicted by this curve. Therefore, it is very interesting for industrials to obtain the residual stress profile of 99% when the effects of inherent uncertainties are significant.

In fact, the developed approach allows the assessment and the control of the shot peening process dispersions. It solves a lot of over-sizing problems of predictive residual stress profile by the generation of iso-probabilistic ones.

References

1. Atig A, Ben Sghaier R, Seddik R, Fathallah R (2017) A simple analytical bending stress model of parabolic leaf spring. Proc IME C J Mech Eng Sci. https://doi.org/10.1177/0954406217709302
2. De la Rosa CEF, Trejo MH, Roman MC et al (2016) Effect of decarburization on the residual stresses produced by shot peening in automotive leaf springs. J Mater Eng Perform 25(7):2596–2603
3. Seddik R, Bahloul A, Atig A, Fathallah R (2017) A simple methodology to optimize shot-peening process parameters using finite element simulations. Int J Adv Manuf Technol 90(5–8):2345–2361
4. Tu F, Delbergue D, Miao H, Klotz T, Brochu M, Bocher P, Levesque M (2017) A sequential DEM-FEM coupling method for shot peening simulation. Surface and Coatings Technology 319:200–212
5. S.T.S Al-Hassani (1981). Mechanical aspects of residual stress development in shot peening, in: Proceedings of the 1st International Conference on Shot Peening, Paris, pp.583–602
6. Fathallah R, Sidhom H, Braham C, Castex L (2003) Effect of surface properties on high cycle fatigue behaviour of shot peened ductile steel. Mater Sci Technol 19(8):1050–1056
7. Fathallah R, Laamouri A, Sidhom H, Braham C (2004) High cycle fatigue behavior prediction of shot-peened parts. Int J Fatigue 26(10):1053–1067
8. Kirk D (2009) Strip factors influencing Almen arc height. Shot Peener 23(4):26–32
9. Kirk D (2011) Variability of a shot stream's measured peening intensity. Shot Peener 25(3):24–32
10. Almen JO, Black PH (1963) Residual stresses and fatigue in metals. McGraw-Hill, Toronto
11. SAE Standard (2008) J442—test strip, holder, and gage for shot peening
12. SAE Standard (2003) J443—procedures for using standard shot peening test strip
13. Atig A, Ben Sghaier R, Seddik R, Fathallah R (2017) Reliability-based high cycle fatigue design approach of parabolic leaf spring. Proc IME L J Mater Des Appl. https://doi.org/10.1177/1464420716680499
14. Kaiser B, Berger C (2005) Fatigue behaviour of technical nsprings. Mater Werkst 36:685–696
15. Chardin H, Slim S, Inglebert G (1996). Modelling the influence of the shot size dispersion on the evolution of the residual stress profiles vs time in shot peening. In: proceedings of the 6th international conference on shot peening (ICSP-6), San Francisco, p.348–355
16. Kirk D (2009) Size and variability of cast steel of shot particles. Shot Peener 23(1):24–32
17. SAE J444, Cast shot and grit size specifications for peening and cleaning, SAE Standards, May 1993
18. Zinn W and Scholtes B (2000). Influence of shot velocity and shot size on Almen intensity and residual stress depth distributions. In 9th International conference on shot peening (ICSP9), No 20, pp. 379–384
19. Fathallah R, Inglebert G, Castex L (1998) Prediction of plastic deformation and residual stresses induced in metallic parts by shot peening. Mater Sci Technol 14(7):631–639
20. Kartal ME, Basaga HB, Bayraktar A (2011) Probabilistic nonlinear analysis of CFR dams by MCS using response surface method. Appl Math Model 35:2752–2770
21. Seddik R, Sghaier RB, Atig A, Fathallah R (2017) Fatigue reliability prediction of metallic shot peened-parts based on Wöhler curve. J Constr Steel Res 130:222–233
22. Nam YS, Jeong YI, Shin BC, Byun JH (2015) Enhancing surface layer properties of an aircraft aluminum alloy by shot peening using response surface methodology. Mater Des 83:566–576
23. Nam YS, Jeon U, Yoon HK, Shin BC, Byun JH (2016) Use of response surface methodology for shot peening process optimization of an aircraft structural part. Int J Adv Manuf Technol 87(9–12):2967–2981
24. Karataş C, Sozen A, Dulek E (2009) Modelling of residual stresses in the shot peened material C-1020 by artificial neural network. Expert Syst Appl 36(2):3514–3521
25. Maleki E, Farrahi GH, Sherafatnia K (2016) Application of artificial neural network to predict the effects of severe shot peening on properties of low carbon steel. In: Öchsner A, Altenbach H (eds) Machining, Joining and Modifications of Advanced Materials. Springer, Singapore, pp 45–60
26. Maleki E, A. Zabi-hollah, Modeling of shot-peening effects on the surface properties of a (TiB + TiC)/Ti-6Al-4V composite employing artificial neural networks, Materiali in tehnologije 50 (2016) 6, 851–860
27. Seddik, R., Petit, E. J., Rabii, B. S., Atig, A., & Fathallah, R. (2017). Predictive design approach of high-cycle fatigue limit of shot-peened parts. The International Journal of Advanced Manufacturing Technology, 1-19
28. Seddik R, Ben Sghaier R and Fathallah R (2016). A numerical–analytical approach to predict the effects of shot peening on the fatigue performance of the nickel-based super alloy Waspaloy. Proceedings of the Institution of Mechanical Engineers, Part L: Journal of Materials: Design and Applications, 1464420716663030
29. Frija M, Hassine T, Fathallah R, Bouraoui C, Dogui A (2006) FEM modelling of shot peening process: prediction of the compressive residual stresses, the plastic deformations and the surface integrity. Mater Sci Eng 426:173–180
30. Taehyung K, Hyungyil L, Minsoo K, Sunghwan J (2012) A 3D FE model with plastic shot for evaluation of equi-biaxial peening residual stress due to multi-impacts. Surf Coat Technol 206:3981–3988
31. Hassani-Gangaraj SM, Cho KS, Voigt HJL, Guagliano M, Schuh CA (2015) Experimental assessment and simulation of surface nanocrystallization by severe shot peening. Acta Mater 97:105–115
32. Hassani-Gangaraj SM, Moridi A, Guagliano M (2014) From conventional to severe shot peening to generate nanostructured surface layer: a numerical study. IOP Conf Ser: Mater Sci Eng 63:012038
33. Bagherifard S, Ghelichi R, Guagliano M (2010) A numerical model of severe shot peening (SSP) to predict the generation of a nanostructured surface layer of material. Surf Coat Technol 204:4081–4090
34. Jebahi M, Gakwaya A, Levesque J, Mechri O, Ba K (2016) Robust methodology to simulate real shot peening process using discrete-continuum coupling method. Int J Mech Sci 107:21–33
35. Guechichi H, Castex L, Frelat J, Inglebert G (1986) Impact surface treatment, vol 11–12. Elsevier, London
36. Khabou MT, Castex L, Inglebert G (1990) The effect of material behaviour law on the theoretical shot peening results. European journal of mechanics. A Solids 9(6):537–549
37. Shen S, Atluri SN (2006) An analytical model for shot peening induced residual stresses. Comput Mater Continua 4(2):75–85
38. Li JK, Mei Y, Duo W, Renzhi W (1991) Mechanical approach to the residual stress field induced by shot peening. Mater Sci Eng A 147(2):167–173
39. Miao HY, Larose S, Perron C, Lévesque M (2010) An analytical approach to relate shot peening parameters to Almen intensity. Surf Coat Technol 205:2055–2066
40. Guechichi H, Castex L, Benkhettab M (2013) An analytical model to relate shot peening Almen intensity to shot velocity. Mech Based Des Struct Mach 41(1):79–99
41. Franchim AS, de Campos VS, Travessa DN, de Moura NC (2009) Analytical modelling for residual stresses produced by shot peening. Mater Des 30(5):1556–1560

42. Davis J, Ramulu M (2015) A study of the residual stress induced by shot peening for an isotropic material based on Prager's yield criterion for combined stresses. Meccanica 50(6):1593–1604
43. Sherafatnia K, Farrahi GH, Mahmoudi AH, Ghasemi A (2016) Experimental measurement and analytical determination of shot peening residual stresses considering friction and real unloading behavior. Mater Sci Eng A 657:309–321
44. Johnson KL (1985) Contact mechanics. Cambridge University Press, Cambridge, UK
45. Ilyushin AA (1948) Plasticity (in Russian). Gostekhizdat, Moscow
46. Guagliano M (2001) Relating Almen intensity to residual stresses induced by shot peening: a numerical approach. J Mater Process Technol 110(3):277–286
47. Cao W, Fathallah R, Castex L (1995) Correlation of Almen arc height with residual stresses in shot peening process. Mater Sci Technol 11(9):967–973
48. Nordin E, Ekström K, Alfredsson B (2014) Experimental investigation of thestrain rate dependence of the SS 2506 gear steel, Int conf on shot peening 12 (ICSP-12) Goslar, Germany
49. Aggarwal ML, Khan RA, Agrawal VP (2005) Investigation into the effects of shot peening on the fretting fatigue behaviour of 65Si7 spring steel leaf springs. Proc IME L J Mater Des Appl 219(3):139–147